Supplementary Materials for

Unconventional route to control the chemical doping of molecular semiconductors through proton-coupled electron transfer in aqueous solutions

Masaki Ishii, Yu Yamashita, Shun Watanabe, Katsuhiko Ariga, and Jun Takeya

Correspondence and requests for materials should be addressed to

Yamashita.Yu@nims.go.jp (Y.Y.)

Contents

1. Supplementary Methods and Discussion.

1.1 Materials and doping methods

The polymeric semiconductor poly[2,5-bis(3-tetradecylthiophen-2-yl)thieno[3,2-*b*]thiophene] (PBTTT) is one of the most widely studied p-type organic semiconductors (OSCs) and is known to exhibit high field-effect mobility. PBTTT, with an estimated molecular weight of 40,000-80,000 Da, was purchased from Sigma-Aldrich and used as received. *o*-Dichlorobenzene (*o*DCB) was purchased from Tokyo Chemical Industry (TCI) and used as a solvent for PBTTT. 1,4-Benzoquinone (BQ) and hydroquinone (HQ) were purchased from TCI as redox agents. Lithium bis(trifluoromethanesulfonyl)imide (LiTFSI) and lithium bis(nonfluorobutanesulfonyl)imide (LiNFSI) were purchased from TCI and used as dopant salts. Sulfuric acid (SA), phosphoric acid (H_3PO_4), potassium dihydrogen phosphate (KH_2PO_4), dipotassium hydrogenphosphate (K_2HPO_4) and acetic acid (CH_3COOH) were used for pH control and purchased from Nacalai Tesque. Potassium hydroxide (PH) and potassium acetate (CH_3COOK) were used for pH control and purchased from FUJIFILM Wako Pure Chemical Corporation. The deionized (DI) water used for solution preparation was distilled and deionized using Purelab Option R7, Flex (ELGA). The molecular structures of main compounds are shown in Figure 1 in the main text.

The PBTTT thin films were fabricated on standard EAGLE XG glass substrates for UV-vis-NIR spectroscopy and XRD analysis and on Cr/Au-patterned and covered EAGLE XG glass substrates for conductivity and potential, XPS, and PYS measurements. The thin films were deposited via spin-coating from a 1 wt% (0.5 wt% for the experiment shown in Fig. 5 in the main text) *o*DCB solution at a spinning speed of 2000 rpm for 1 min. The resulting films were annealed in a vacuum oven at 180 °C for 1 h and then cooled slowly to room temperature. The film thickness was determined to be 42 ± 2 nm using a Dektak surface profilometer. The PBTTT films were washed with DI water and then doped by immersion in aqueous dopant solutions at room temperature. The doping solutions were prepared by dissolving BQ, HQ and/or dopant salts in pH-controlled aqueous solutions. After 20 min of immersion, the films were removed from the solution, and the residual solvent was blown away by a N_2 flow. The detailed conditions of the solution preparation processes are listed in Table S1-S4. All doping (immersion) processes were performed under ambient conditions, and the films obtained were subjected to several measurements under

atmospheric conditions.

solution name	redox agent	salt
BQ-LiNFSI	BQ 50 mM	LiNFSI 4 mM
BQ-LiTFSI	BQ 50 mM	LiTFSI 100 mM
LiNFSI	—	LiNFSI 4 mM
LiTFSI	—	LiTFSI 100 mM
BQ	BQ 50 mM	—

Table S1: Solution preparation conditions for the experiment shown in Fig. 1 in the main text.

solution name	redox agent	salt	buffer (10 mM)
pH 2	BQ 10 mM, HQ 10 mM	LiTFSI 100 mM	H_3PO_4-KH_2PO_4
pH 4	BQ 10 mM, HQ 10 mM	LiTFSI 100 mM	CH_3COOH-CH_3COOK

Table S2: Solution preparation conditions for the experiment shown in Fig. 4 in the main text. The total solution volume was 5 mL.

solution name	redox agent	salt
BQ-LiNFSI	BQ 50 mM	LiNFSI 1 mM
BQ-LiTFSI	BQ 50 mM	LiTFSI 100 mM
DDQ-LiNFSI	DDQ 2 mM	LiNFSI 1 mM
DDQ-LiTFSI	DDQ 2 mM	LiTFSI 100 mM

Table S3: Solution preparation conditions for the experiment shown in Fig. 5 in the main text.

solution name	redox agent	salt	buffer (10 mM)
pH 1	BQ 10 mM, HQ 1 mM	LiNFSI 1 mM	—
pH 2	BQ 10 mM, HQ 1 mM	LiNFSI 1 mM	H_3PO_4-KH_2PO_4
pH 3	BQ 10 mM, HQ 1 mM	LiNFSI 1 mM	H_3PO_4-KH_2PO_4
pH 4	BQ 10 mM, HQ 1 mM	LiNFSI 1 mM	CH_3COOH-CH_3COOK
pH 5	BQ 10 mM, HQ 1 mM	LiNFSI 1 mM	CH_3COOH-CH_3COOK
pH 6	BQ 10 mM, HQ 1 mM	LiNFSI 1 mM	KH_2PO_4-K_2HPO_4
pH 7	BQ 10 mM, HQ 1 mM	LiNFSI 1 mM	KH_2PO_4-K_2HPO_4

Table S4: Solution preparation conditions for the experiment shown in Extended Data Fig. 4

1.2 Characterization of doping

UV-vis-NIR spectroscopy. The UV-vis-NIR spectra of the thin films were acquired from specimens on glass substrates in air using a JASCO spectrometer (V-670).

X-ray diffraction (XRD) measurement. Out-of-plane and in-plane XRD data were acquired using a RIGAKU SmartLab with a MicroMax-007HF X-ray generator using Cu Kα radiation ($\lambda = 0.15418\,\mathrm{nm}$) in conjunction with a 0.1 mm-thick EAGLE XG glass substrate to reduce substrate scattering. For the out-of-plane direction, $\theta - 2\theta$ method was employed. For in-plane direction, data was acquired by converting two dimensional wide angle x-ray scattering images. In particular, XRD spectra of PBTTT thin films in the in-plane direction shown in Fig. 2e in the main text come from Fig. S1.

According to the XRD measurements, no apparent changes in morphology were observed before and after doping, *i.e.*, the terrace structure due to the microcrystalline and lamellar nature of PBTTT was maintained even after doping. In addition, because neither significant broadening nor splitting was observed in the diffraction peaks, the incorporation of the dopant was homogeneous over the entire bulk of the PBTTT thin film.

Photoelectron yield spectroscopy (PYS) measurement. PYS data were obtained from thin films on Cr/Au-coated glass substrates using a SUMITOMO PYS-202 instrument.

Electrode potential measurement. A PBTTT thin-film electrode was prepared on a Cr/Au-patterned glass substrate by blade coating[1] with a shearing rate of $100\,\mu\mathrm{m\,s^{-1}}$ from a 0.5 % *o*DCB solution. The electrode potential of PBTTT was measured from a system in which a Ag/AgCl electrode was used as the reference electrode, as shown in Extended Data Fig. 2a. The aqueous solutions used were composed of the BQ/HQ redox couple (10 mM) and LiTFSI (100 mM). SA and PH were used for pH control.

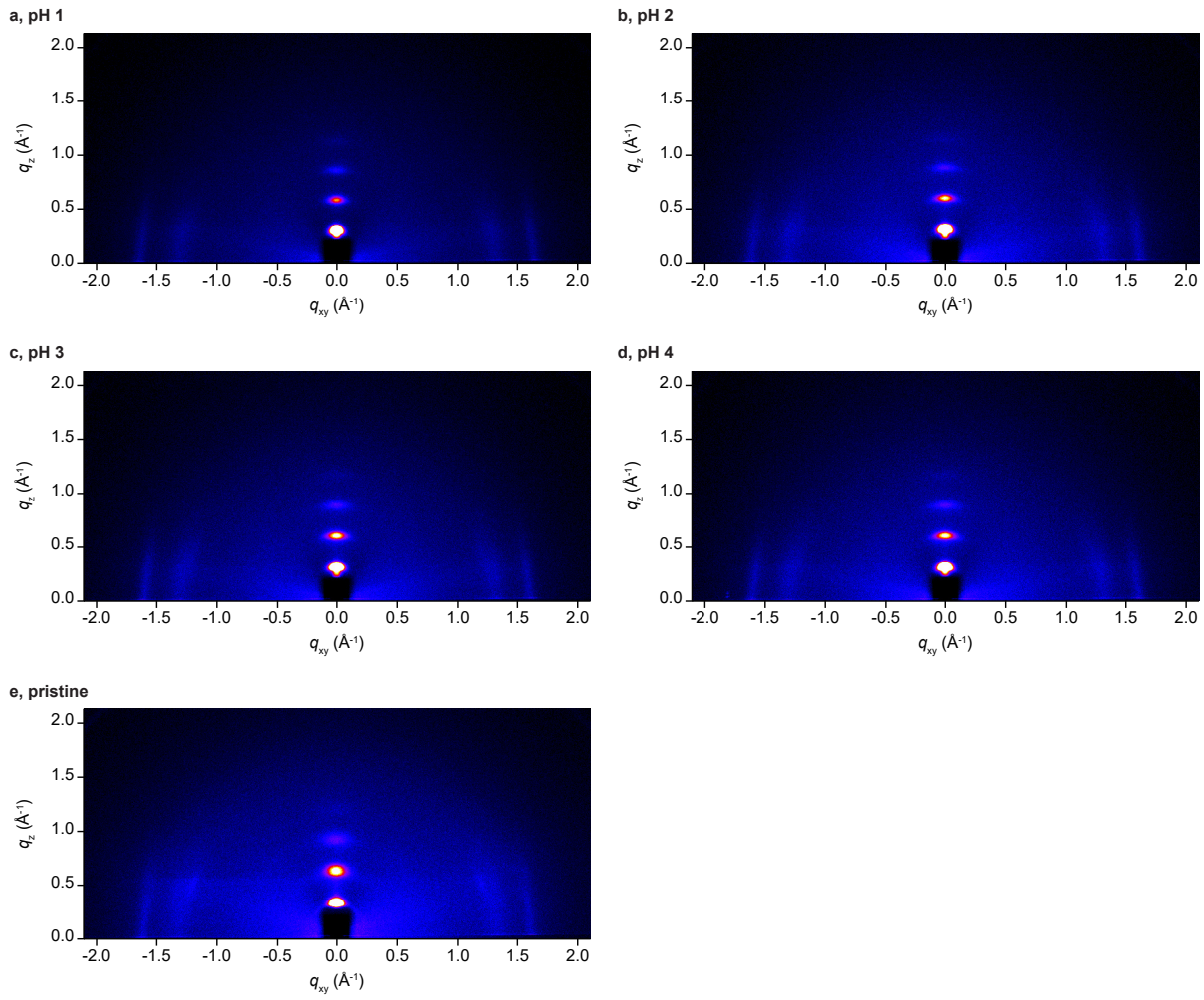

Figure S1: Wide angle x-ray scattering images of PBTTT thin films immersed in aqueous solutions with BQ/HQ (both 10 mM) and LiTFSI (100 mM) at pH 1-4. The images were used for structural analyses especially in the in-plane direction (Fig. 2e in the main text).

1.3 Effect of dissolved oxygen

The equilibrium reaction of oxygen evolution shown in the Pourbaix diagram (Fig. 1b in the main text) is described as follows.

$$2\,H_2O\,(liq) \rightleftharpoons O_2(g) + 4\,H^+ + 4\,e^- \tag{S1}$$

A high proton concentration promotes a leftward shift of the equilibrium when oxygen and electrons exist; that is, dissolved oxygen in aqueous solution may oxidize OSCs at low pH. In this section, we assessed whether dissolved oxygen perturbs the precise control of the doping level by a BQ/HQ redox couple. Extended Data Fig. 1a shows the conductivities of PBTTT thin films immersed in aqueous solutions with LiTFSI at 100 mM. The conductivity increased with decreasing solution pH, which was derived from oxidation by dissolved oxygen as a substitute for BQ/HQ. Note that the equilibrium of Equation (S1) is inclined to the right because our doping system consisted of a large amount of water. Considering that the oxygen amount in pure water is $8.11\,mg\,L^{-1}$ at 25 °C and 1 atm[2], the molecular ratio of water to oxygen is estimated to be 2.2×10^5. Therefore, the reduction reaction proceeds to a limited extent when the proton concentration is high, and a dopant anion prevents the reverse reaction. In fact, the increase in conductivity is significant when BQ is used as an oxidant instead of dissolved oxygen; for instance, the conductivity of the system may increase by as much as ca. 20000 times at pH 1. In addition, the effect of dissolved oxygen could be neglected by Ar bubbling (Extended Data Fig. 1b).

1.4 Analysis of the X-ray photoelectron spectra

X-ray photoelectron spectroscopy (XPS) was employed to evaluate the atomic composition of the doped PBTTT films. XPS was performed using a KRATOS ULTRA 2 instrument with monochromatic Al Kα X-rays.

In the main text, we focused on the C 1s and F 1s spectra of $TFSI^-$ doped PBTTT thin films to determine the F/C atomic ratio. The XPS narrow spectra of other atoms are described here to further describe the atomic composition of the doped PBTTT films (Fig. S2). The atomic amounts of O and N increased with decreasing solution pH, thus suggesting that $TFSI^-$ was effectively introduced into the films based on our doping model. The increase in the intensity of the sulfone peak at pH 1 also supported the intercalation of $TFSI^-$ into the PBTTT thin film.

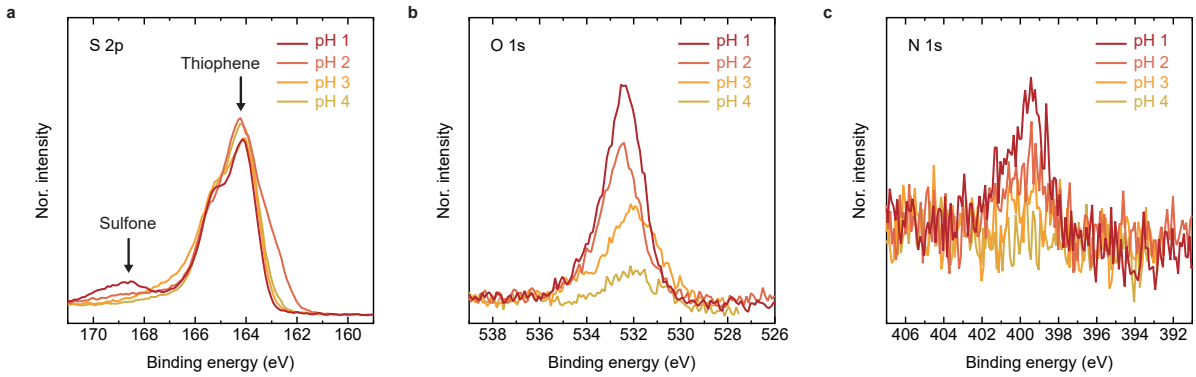

Figure S2: XPS narrow spectra of the S 2p (a), O 1s (b) and N 1s (c) regions of the same PBTTT thin films shown in Fig. 3b-d in the main text.

1.5 Application of our method to a wide pH range

The doping efficiency of our method depends on several factors, such as the ionization potential (IP) and electron affinity (EA) of the materials and the interactions between the solid OSC and dopant anion. Thus, we can prepare OSC materials with the desired carrier density or IP by changing these parameters. In this section, we demonstrate pH-dependent conductivity changes over a wide pH range, from the neutral region, as an application of our doping method. Poly(3-hexylthiophene-2,5-diyl) (P3HT) was purchased from Sigma-Aldrich and used as a p-type OSC instead of PBTTT because of its lower IP. UV-vis-NIR spectroscopy and conductivity measurements (Extended Data Figs. 4a,b) showed that the doping level of P3HT was controlled by the solution pH, similar to the doping level of PBTTT shown in the main text. The doping reaction did not significantly disrupt the intrinsic crystalline structure of P3HT. Changes in d-spacing imply that dopant anions were intercalated between the layers of the lamellar structures by our doping method (Extended Data Figs. 4c,d). These results could lead to the development of a new type of resistive-based pH sensor. A system that does not require a bulky reference electrode and affords simple resistive measurements would contribute to the miniaturization of pH sensors.

2. Supplementary References

[1] Yamamura, A. *et al.* Wafer-scale, layer-controlled organic single crystals for high-speed circuit operation. *Science advances* **4**, eaao5758 (2018).

[2] Truesdale, G. & Downing, A. Solubility of oxygen in water. *Nature* **173**, 1236–1236 (1954).